

GASL TR384

Environmentally-Neutral Aircraft Using Low-Temperature Plasmas  
NIAC Phase I Final Report

Prepared For

NASA Institute for Advanced Concepts  
Dr. Robert Cassanova, Director  
Universities Space Research Association  
Atlanta, GA 30318

Prepared Under

Grant Number 07600-048

Prepared By

J. C. Leylegian, J. S. Tyll, and W. Chinitz

GASL, Inc.  
77 Raynor Avenue  
Ronkonkoma, NY 11779-6648

November 2000

Approved By:

---

Jason S. Tyll  
Program Manager

---

Wallace Chinitz  
Chief Scientist

## **Abstract**

To determine the feasibility of developing a system using plasma generation for NO<sub>x</sub> reduction from gas turbine exhaust, a plasma reactor was built and tested using products of an ethylene/air reactant premixture. Gas chromatography (GC), mass spectroscopy (MS), and ultraviolet lamp absorption measurements were taken to determine the reduction of nitric oxide (NO) in the exhaust gases between plasma-on and plasma-off conditions. Using the fan-type plasma generator at the University of Connecticut, in conjunction with the combustor built for this study, independent GC and MS measurements showed decreases in the NO concentrations of 15 to 30% with plasma generation, while also showing a 7% increase in nitrogen dioxide (NO<sub>2</sub>) concentration. Given the time and budgetary constraints, it was not possible to run the plasma generator at GASL, but absorption measurements were taken for combustion products and for air. The power of the transmitted light dropped by over 50% when the combustor was running, suggesting that UV light absorption by NO should be easily detectable for this experimental setup.

## Table of Contents

Abstract .....	2
List of Figures .....	4
Introduction .....	5
Experimental Methodology .....	7
Ethylene/Air Combustor .....	7
All-Quartz Plasma Generator .....	7
Fan-Type Plasma Generator .....	8
UV Absorption Measurements .....	8
Gas Chromatography and Mass Spectroscopy .....	9
Results and Discussion.....	10
University of Connecticut Experiments .....	10
GASL Experiments .....	11
Conclusions .....	12
Recommendations.....	12
Acknowledgments.....	14
References .....	22

## List of Figures

Figure 1: Photographs of the experimental setups. Upper: setup as used at GASL. Lower: setup as used at the University of Connecticut. ....	15
Figure 2: Photograph of the ethylene/air combustor used in this work (scale in inches).	16
Figure 3: Schematic of the ethylene/air combustor.....	16
Figure 4: All-quartz tubular reactor, shown with Inconel electrodes (scale in inches). ...	17
Figure 5: Schematic of the all-quartz tubular reactor. ....	17
Figure 6: Fan-type plasma reactor (white box on right) shown with Japan-Inter uHV-10 AC power source and Yokogawa digital oscilloscope DL 1520, as used in experiments conducted at the University of Connecticut. ....	18
Figure 7: Fan-type plasma reactor removed from outer casing (scale in inches). ....	18
Figure 8: Waveform employed in fan-type plasma generator experiments. Waveform image was acquired from a Yokogawa digital oscilloscope DL 1520 used to monitor the setup. ....	19
Figure 9: Configuration used for UV absorption measurement. ....	19
Figure 10: Schematic of modifications made to the combustor exit to avoid combustor instabilities during the experiments performed at the University of Connecticut. ....	20
Figure 11: GC output data. Upper: data for plasma-off condition. Lower: data for plasma-on condition. Arrows are pointing to the peak corresponding to NO effusion from the GC column. Scales of the two plots are identical. ....	20
Figure 12: MS results for plasma-off and plasma-on conditions, including NO, NO <sub>2</sub> and NO <sub>x</sub> (NO + NO <sub>2</sub> ). ....	21
Figure 13: Paschen curve, relating required breakdown voltage to gas pressure times gap width for a typical gas. Both scales are logarithmic. Plot adapted from Ref. [19].....	21

## Introduction

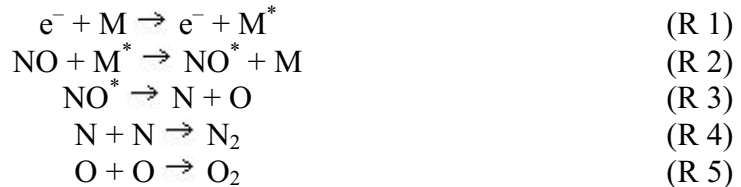
The formation and release of nitrogen oxides ( $\text{NO}_x$ ) into the environment is a consequence of hydrocarbon combustion in both stationary and mobile power plants. In 1968, the transportation and stationary power plants accounted for almost 90% of the  $\text{NO}_x$  emissions in the United States [1]. The two main nitrogen oxide compounds that are released by these sources are nitric oxide (NO) and nitrogen dioxide ( $\text{NO}_2$ ). These compounds are hazardous to human health, as well as to the environment at large.  $\text{NO}_2$ , which is emitted directly from engines, as well as formed through reactions of NO with oxygen in the atmosphere, is a severe respiratory irritant, and can react with moist air to form nitric acid ( $\text{HNO}_3$ ), a corrosive agent. In addition,  $\text{NO}_x$  is a key player in photochemical smog reaction cycles [1, 2]. As a result, technologies that would significantly reduce the levels of  $\text{NO}_x$  emissions from such power sources have been sought for years.

The 1990s saw considerable activity in the area of  $\text{NO}_x$  reduction from combustion sources. The ubiquitous use of rhodium in automotive catalysts stems from its high activity and selectivity for NO reduction to  $\text{N}_2$ , coupled with its ability to withstand harsh operating environments. Rhodium's high selectivity for NO, which is markedly superior to other noble metals, such as platinum and palladium, stems from its ability to promote N-pairing in adsorbed NO molecules before the N-O bond is broken [3]. However, rhodium is the most costly active metal used in automotive pollution control devices and is becoming increasingly difficult to obtain.

Much work has centered on the use of hydrocarbons in the presence of  $\text{O}_2$  to selectively reduce  $\text{NO}_x$  over copper [4, 5], iron [6], and zeolite [7] catalysts. From the viewpoint of the aircraft design engineer, this approach has many drawbacks. Among these are the added lift requirements associated with carrying excess fuel and/or reductant hydrocarbon, the requirement for a suitable catalytic material, the production of unburned and partially burned hydrocarbons in the exhaust gas, which will increase carbon monoxide (CO), and the reduction in  $\text{NO}_x$ -reducing ability in the presence of water vapor [7]. The direct decomposition of  $\text{NO}_x$  using catalysts has also seemingly struck an impasse over the inability to find an effective catalyst that remains stable in the presence of water vapor [7].

Keeping in mind the drawbacks of the methods presented above, the long-term need is clear for a relatively inexpensive way to reduce  $\text{NO}_x$  without negatively affecting other environmental control measures. The recent work of Luo *et al.* [8, 9] using low-

temperature plasmas to decompose  $\text{NO}_x$  in helium represents a promising approach to this problem from the viewpoint of the turbojet engine (or any other mobile power plant for that matter) designer. “Low-temperature” implies plasma excitation temperatures in the range of 3000-5500 K; however, wall temperatures are unaffected by the presence of the plasma at low pressures (1 atmosphere or less). The NO conversion reaction is believed to occur via the following mechanism [8]:



In the reactions listed above, the asterisk indicates an excited species. The presence of energetic electrons helps activate the bath gas molecules, which in turn collide with NO molecules, causing their rupture and subsequent recombination to form  $\text{N}_2$  and  $\text{O}_2$ . Such a scheme could be accelerated if the bath gas is composed of diatomic molecules that are more easily activated than monatomic gases, and/or a gas with lower ionization energy. In the case of lean combustion products, the main component is  $\text{N}_2$ , which has an ionization energy of 15.51 eV, versus 24.46 eV for He.

However, this study also shows some potential drawbacks in the adaptation of this phenomenon to engine exhaust treatment. For instance, it was shown that the addition of 5.5% carbon dioxide ( $\text{CO}_2$ ) or 3.2% water vapor ( $\text{H}_2\text{O}$ ) to 0.45% NO in helium at room temperature decreases the conversion of NO. Since the products of hydrocarbon combustion contain both of these species at levels comparable to those investigated in the aforementioned study, the effectiveness of this approach to NO removal must be demonstrated. However, it must also be noted that the previous study [8] was conducted at room temperature, while the temperature of combustion products from a turbojet engine can be as high as 1700 K [10]. Elevated temperatures could possibly accelerate the NO conversion reaction through increased collision rates.

In this report we will present our preliminary findings on the use of this technology for removal of  $\text{NO}_x$  from a simulated jet exhaust stream. To perform these experiments, initially at atmospheric pressure, a bench-scale combustion chamber was built to run on ethylene-air mixtures at fuel/air ratios comparable to those encountered in a typical turbojet engine. For on-site experiments, an all-quartz tubular plasma generator was designed and built, and for experiments conducted at the University of Connecticut, a plasma generator used in several previous studies was used in conjunction with the GASL-designed combustion chamber.

## Experimental Methodology

The entire flow system used in the experiments conducted at GASL can be seen in the upper panel of Fig. 1. Ethylene and air were metered using Cole-Parmer rotameters, and passed through flashback arrestors to prevent backflow of gas in the event of flame flashback. The gases were mixed and entered a combustion chamber in which the fuel was burned, and the exhaust gases were then sent through an all-quartz tubular plasma generator. The final products were examined using a UV light absorption apparatus. The experiments conducted at the University of Connecticut, illustrated in the lower panel of Fig. 1, were conducted in a similar manner. The main differences were that the fan-type reactor used in previous studies [13] was used to generate the plasma, and gas chromatography and mass spectrometry were used to analyze the products.

### *Ethylene/Air Combustor*

A photograph and a schematic of the stainless steel atmospheric pressure combustor used in this study can be seen in Figs. 2 and 3, respectively. The combustor, designed and built at GASL for this study, is essentially a Bunsen burner in a pipe, with additional air added at the walls and mixed in with the flame products downstream of the flame, a process that is similar to what occurs in an actual jet engine. This configuration has two advantages. First, the jacket air cools the outside of the combustor. Second, the air lowers the exit temperature of the gas below the 1700 K limit imposed by the materials used in a typical turbojet engine [10], without attempting to stabilize a flame that is close to the lean flammability limit of ethylene ( $C_2H_4$ ), the fuel used in this study. The fuel/air mixture was ignited using a spark ignition system powered by a 10 kV autotransformer. In the GASL experiments, the combustor and reactor were connected directly, while in the experiments conducted at the University of Connecticut, an adapter was fabricated to direct the product gases to the fan-type plasma reactor.

### *All-Quartz Plasma Generator*

In Ref. 8, all-quartz tubular reactors have shown good activity for NO removal, as well as excellent stability. Subsequent work [12–14] has demonstrated the uses for alternative plasma reactor configurations. In this study, two different plasma generators were used. Figures 4 and 5 show a photograph and a schematic, respectively, of the all-quartz tubular reactor used in experiments performed at GASL. The term “all-quartz” refers to the fact that in this configuration, the wetted surfaces are quartz, rather than the electrode materials. This was done both here and in previous studies [8] to avoid any catalytic reactions of the combustion products resulting from contact with the electrode

metal, thereby isolating the effect of the low-temperature plasma. To withstand the high temperatures encountered in this experiment, the electrodes were constructed of Inconel, rather than the copper and aluminum used in Ref. 8, due to the higher melting point of Inconel. After passing through the reactor, the gas exits upward through a slotted tube covered by a quartz sleeve. This is an optical port used for an absorption measurement setup, described below. The annulus has an inside diameter of 8.85 mm, and an outside diameter of 9.75 mm. The reactor is 90 mm long, yielding a volume of 1.183 cm<sup>3</sup>.

The plasma generator is powered by a solid-state induction coil, manufactured by Electro-Technic Products. This coil is capable of producing a pulsating (7.1 kHz) DC voltage ranging from 15 to 45 kV, with current up to 50 mA, depending upon the load. Leads connecting the power supply to the plasma generator were constructed from automotive ignition wire, rated for 55 kV and current as high as 750 mA.

#### *Fan-Type Plasma Generator*

As mentioned above, a fan-type plasma generator [11–13] was used in the experiments conducted at the University of Connecticut. Figure 6 is a photograph of the fan-type reactor setup, along with the power source and oscilloscope. Figure 7 is the reactor removed from its Teflon casing. The rotor (inner disk) and stator (outer ring) serve as the electrodes. Both rotor and stator were coated with iron using electroless plating. The rotor has a diameter of 5.59 cm, a width of 1.66 cm, and ten evenly spaced fan blades, which protrude 0.34 cm from the rotor. The stator has an inner diameter of 6.33 cm, producing a gap width of 0.3 mm. The rotor is driven by an electric motor that rotates at speeds up to 3600 rpm. The fan motor was on during both plasma-off and plasma-on experiments. The total volume of the reactor, including dead space both upstream and downstream of the fan, is 200 cm<sup>3</sup>.

The plasma generator is powered by a Japan-Inter uHV-10 AC high-voltage generator operating at 8.1 kHz with a non-conventional waveform, shown in Fig. 8. This is the same power supply used in previous studies performed at the University of Connecticut [8, 9, 11–15]. The electrical output was monitored using a Yokogawa digital oscilloscope DL 1520. Experiments were conducted at a voltage of 2 kV, and a frequency of approximately 8 kHz.

#### *UV Absorption Measurements*

Three different methods were used to determine the difference in NO<sub>x</sub> levels between plasma-on and plasma-off conditions. The method used in the GASL

experiments was an ultraviolet light absorption method, illustrated in Fig. 9. This method has been used successfully in the measurement of NO in flow reactor studies at Princeton University [16]. This method determined NO levels by monitoring the absorption from the  $A^2\Sigma^+ \leftarrow X^2\Pi(0,0)$  band, which has a peak at a wavelength near 226 nm. A deuterium lamp was used as the light source in this measurement. The light was collimated and directed to the optical port on the plasma generator using a fiber optic cable. The light was collected after passing through the optical port, and directed into a spectrometer using another fiber optic cable. The spectrometer used in this work is identical to the one used by Lempert [17] for OH absorption measurements. The light exiting the spectrometer is sent to eight photomultiplier tubes (PMTs), with each PMT detecting light at a slightly different wavelength. In this way, a spectrum covering approximately 10 nm can be assembled instantaneously, instead of having to scan over a range of wavelengths.

The PMT output is an electric current, which can be converted into a light intensity for a given PMT. Changes in light intensity for different gas compositions are due to light absorption by gas constituents undergoing ro-vibrational or electronic transitions. The absorption data can then be used to determine the NO concentration in the gas sample. The Beer-Lambert law relates intensity to sample concentration and sample thickness [18]:

$$\log \frac{I_o}{I} = A = \varepsilon(\lambda, T)pl \quad (1)$$

where  $I_o$  and  $I$  are the intensities measured for the reference gas and the sample gas; respectively;  $\varepsilon$  is the absorption coefficient, which is a function of wavelength  $\lambda$  and temperature;  $p$  is the partial pressure of the species of interest in the sample; and  $l$  is the thickness of the gas sample. If  $\varepsilon$  is known for all  $\lambda$  and  $T$ , the concentration of the gas of interest can be calculated directly. If not, qualitative measurements can still be made, since the intensity of light transmitted (and therefore the PMT output signal) will decrease with an increase in NO concentration.

For the setup used in this work, the PMT current was converted to a voltage using a 50  $\Omega$  terminator. In addition, the signal was conditioned with a 1.06 kHz low-pass filter, built in-house.

### *Gas Chromatography and Mass Spectroscopy*

Two independent methods to measure NO<sub>x</sub> levels were used in the experiments conducted at the University of Connecticut. The first method was gas chromatography.

A Hewlett-Packard Model 5990A gas chromatograph (GC) was used, equipped with a thermal conductivity detector (TCD) and a Carboxen 2000 column. Helium was used as the carrier gas.

The second method used was mass spectroscopy. In particular, an MKS-UTI PPT quadrupole residual gas analyzer mass spectrometer (MS) was used with a Faraday cup detector and a variable high pressure sampling manifold. Data were collected at  $m/Z$  values of 18, 28, 30, 32, 44, and 46, which were used to monitor the levels of H<sub>2</sub>O, N<sub>2</sub>, NO/NO<sub>2</sub>, O<sub>2</sub>, CO<sub>2</sub>, and NO<sub>2</sub>, respectively. The MS data were used to confirm that the burner was lit, as well as to measure NO<sub>x</sub> levels in the exhaust.

## Results and Discussion

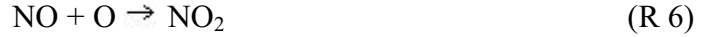
### *University of Connecticut Experiments*

Experiments were conducted at the University of Connecticut, using the fan-type plasma reactor discussed above and in previous studies [11–13]. The combustor was run at an overall equivalence ratio of 0.45. There were some difficulties encountered in keeping the combustor lit while maintaining a connection to the plasma generator and the diagnostic equipment. The combustion products exited the chamber through an opening designed to accommodate a ¼" tube. This relatively small opening led to instability in the combustor flow, causing a pressure increase and subsequent flashback and extinction of the flame. To remedy this, only a portion of the flow was sent to the plasma generator; however, the flow was not metered, so this flow rate cannot be accurately determined. A schematic of the modified setup is in Fig. 10.

As mentioned earlier, both GC and MS were used to measure NO<sub>x</sub> levels in the exhaust gases in these experiments. Figure 11 shows the GC data collected for plasma-on and plasma-off conditions. Both plots have the same scale. The arrow on each plot is pointing to the peak corresponding to NO effusion from the GC column. Direct measurement of the heights of the peaks on the two plots shows a drop of 30% in the NO peak when the plasma is turned on, *corresponding to an estimated drop in the NO concentration of 30%*.

Figure 12 compares the data collected by the MS for plasma-on and plasma-off conditions. Since the MS was able to collect data corresponding to the presence of both NO and NO<sub>2</sub>, results for each species are shown, along with their sum, assumed to be the total NO<sub>x</sub> content in the exhaust. The results show a decrease of 17% in NO concentration and a 10% decrease in NO<sub>x</sub> concentration. This difference results from a

7% increase in NO<sub>2</sub> concentration. This phenomenon is not unexpected. The presence of NO<sub>2</sub> as an intermediate in the destruction of NO was seen in previous studies [8, 9], and is most likely due to the reactions



Reaction (R 6) proceeds due to plasma generation, while (R 7) can occur in the absence of plasma generation, and is a pathway for NO<sub>2</sub> formation in air. NO<sub>2</sub> is then converted back to NO via



It has been demonstrated [8, 9] that increasing the voltage and/or residence time could decrease NO<sub>2</sub> levels by allowing additional time for reactions (R 8) and (R 5) to convert NO<sub>2</sub> back to NO.

### *GASL Experiments*

In the experiments conducted at GASL, the same combustor instability was encountered. However, due to the differences in the hardware configurations between these tests and those at the University of Connecticut, no flow bypass could be implemented. As a result, the combustor output was a mixture of burned products and unburned pre-mixture resulting from the oscillation between burning and non-burning conditions. In addition, since activating the plasma generator with unburned fuel flowing through it would be a potential ignition risk, no experiments could be run at GASL at plasma-on conditions while running the combustor. Design changes are planned to allow steady burner operation with the plasma generator installed, although these could not be carried out within the time frame of the Phase I effort.

Since plasma experiments could not be run, we decided to take this opportunity to test the absorption setup. Since we are still searching for a model describing the absorption characteristics of NO, the absorption coefficient  $\epsilon(\lambda, T)$  for NO was not known, and therefore the drop in PMT signal in the presence of NO could not be converted into a partial pressure. A test was conducted, comparing the output from one PMT for air to that for the combustion products. The mixture of fuel and air used in this test yielded a primary flow equivalence ratio of 0.49, a total equivalence ratio of 0.34, and a NO mole fraction of  $4 \times 10^{-4}$ , assuming the primary flow reaches thermodynamic equilibrium and the secondary air flow dilutes the combustion products. For the band 223.1–224.3 nm, the light intensity detected by the PMT dropped from 0.42  $\mu\text{W}$  to 0.20  $\mu\text{W}$ , a drop of 52%. The multimeter used to measure the PMT output has a resolution of

$\pm 0.1$  mV, which is equivalent to  $0.002 \mu\text{W}$  of light intensity. Therefore, such a drop in the light intensity is easily detectable by the setup used in this study.

## **Conclusions**

In this work, a combustor and plasma generator were designed and built, for the purpose of determining whether generating a plasma in the lean products of hydrocarbon combustion could lead to reduction of nitrogen oxide emissions. Two sets of experiments were performed, one at GASL using the setup specifically built for this study, and one at the University of Connecticut using a fan-type plasma generator used in previous studies of plasma-induced chemistry. Experiments at the University of Connecticut showed through independent gas chromatography and mass spectrometry measurements that NO and gross NO<sub>x</sub> concentrations were reduced during plasma generation by 17% and 10% respectively, but that NO<sub>2</sub> concentrations increased slightly. On the basis of these results, we believe that low-temperature plasma generation can be developed into an effective system for NO<sub>x</sub> reduction in mobile power plant exhaust. While the preliminary tests at GASL could not examine the feasibility of the concept, a test of the absorption setup was conducted. The GASL setup will be modified to allow steady combustion with the plasma generator installed.

## **Recommendations**

Now that the concept has been proven, additional effort should be devoted to improving the bench-top rig. One step would be to modify the burner to run at higher pressures. The experiments done here were all performed at atmospheric pressure. In real turbojet combustors, the operating pressures are much higher, at least 5 to 10 atmospheres. The modifications to the combustor itself would not be difficult. The walls of the current burner can withstand a pressure of 3840 psi (260 atm), far above any requirements for this type of research. The end caps would have to be modified to withstand the higher pressure, allowing for larger fasteners to shoulder the higher loads, and appropriate sealing material must be applied to the mating parts to hold pressure.

The rotameters used to measure flow rates for this rig can only withstand 200 psi. If the combustor were to be upgraded to run at 10 atmospheres (150 psi), this setup would no longer be acceptable. Therefore, an alternate method would be necessary for safe and accurate metering of the flow. The use of choked orifices, which is only limited by the pressure of the compressed gas bottles used to supply the system, is one possibility.

Based on the results in this study, along with the work done by Prof. Suib's research team [8, 9, 11–15], further work must be done to refine the design of the plasma generator for use in this particular application. For instance, two different types of reactors were used in this study: an annular reactor and a fan-type reactor. Both have advantages and shortcomings. For instance, the annular reactor is relatively simple to construct and has no moving parts. However, the passage of gas over considerable lengths through tight constrictions can lead to significant pressure losses, which would lead to decreased thermodynamic efficiency of the engine. In addition, at higher pressures, the maximum gap width necessary to cause breakdown of the gas at a given voltage would decrease exponentially according to the Paschen curve, shown in Fig. 13. For this reason, it becomes apparent that plasma generators that work well at atmospheric pressure may not work well at elevated pressures, and as such, further development may be necessary to realize such an instrument. In addition, there is a possibility that placing the generator between the combustor and turbine would be too difficult, and an alternate solution would need to be considered, such as placing it after the turbine. In this case, the working fluid is at much lower pressure, and therefore electrical breakdown of the gas would be easier to achieve.

If the plasma generator were to be operated at atmospheric pressure, an on-board generator may *not* be necessary. Much of the  $\text{NO}_x$  produced by aircraft engines is emitted during idle or high load conditions, which are usually encountered during take-off and landing. Therefore, the highest  $\text{NO}_x$  levels would be encountered at or near airports. A portable unit, placed on the exhaust nozzle during engine idle, could minimize emissions during loading and unloading of the craft. In addition, stationary air scrubbers in the vicinity of the airport could run continuously, removing  $\text{NO}_x$  from the ambient air. Since neither concept is carried on the aircraft, no losses in performance due to added aircraft weight would be encountered. It is clear then that a substantial effort will be required to develop the system architecture that will ultimately be required.

At the current time, only qualitative measurements of NO partial pressures are possible, since the absorption coefficient in Equation (1) is unknown. In order to make quantitative measurements, a database will have to be built or acquired on NO absorption coefficients. Such information can be obtained through experiment, by flowing NO at a known concentration and temperature through the system and recording the resulting PMT output. Since the measurements will be done at elevated temperatures, a heater will be needed to achieve the required conditions.

In previous studies, *e.g.* [8], the effects of input voltage on NO conversion were investigated. However, it is not clear whether the voltage or the current, which is dependent upon the input voltage and is system-specific, is the relevant parameter. Since the initiation reaction involves the collision of an electron with another species, the concentration of electrons, *i.e.*, the current density, may be the fundamental parameter controlling the reaction. By adding load to the generator circuitry and adjusting the source voltage, the effects of varying current and voltage independent of each other, on the conversion of NO could be determined.

### **Acknowledgments**

The authors would like to thank Prof. Steven Suib of the University of Connecticut for giving us the opportunity to test our combustor with his plasma generator, and his students and staff for their assistance in experimentation. This work was funded by the NASA Institute for Advanced Concepts, under grant number 07600-048.

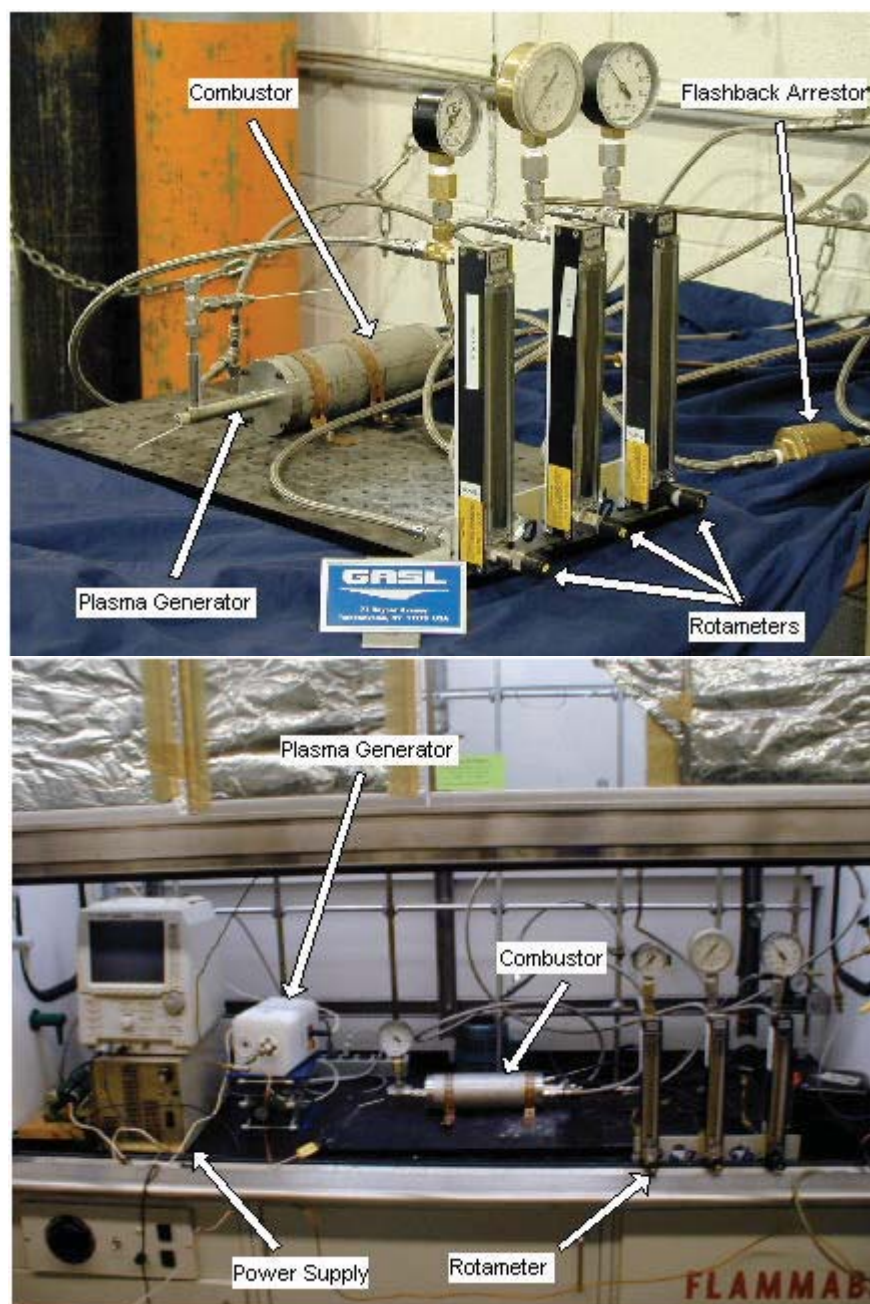
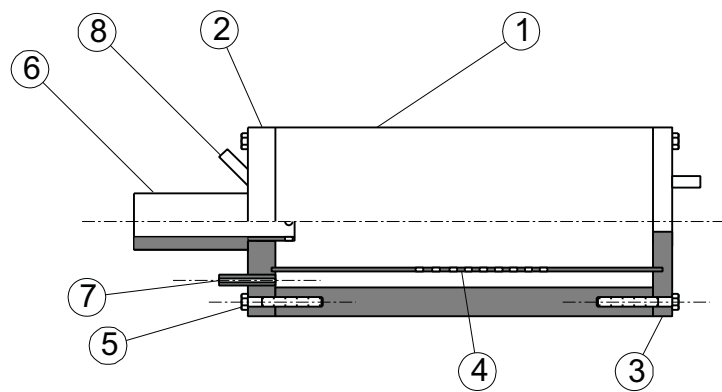


Figure 1: Photographs of the experimental setups. Upper: setup as used at GASL. Lower: setup as used at the University of Connecticut.



Figure 2: Photograph of the ethylene/air combustor used in this work (scale in inches).

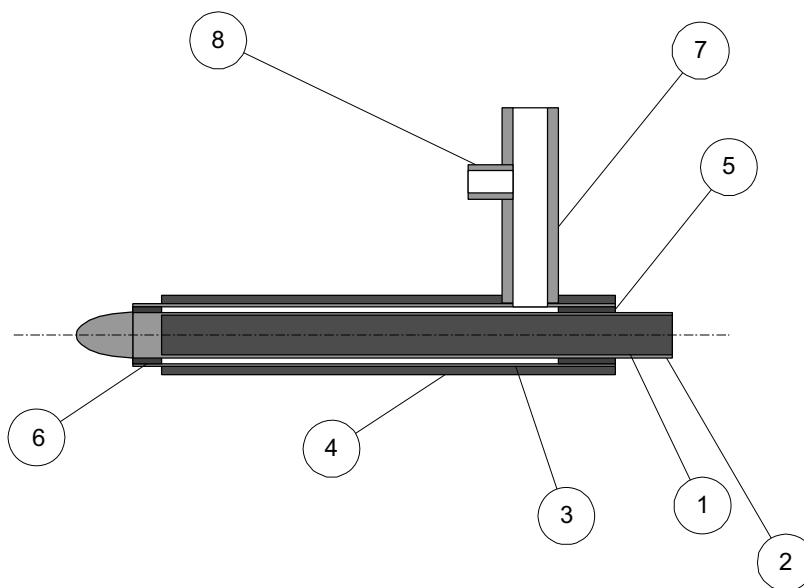


- |                  |                  |                              |                         |
|------------------|------------------|------------------------------|-------------------------|
| 1. body          | 2. front end cap | 3. rear end cap              | 4. jacket air partition |
| 5. machine screw | 6. burner tube   | 7. jacket air injection site | 8. ignition port.       |

Figure 3: Schematic of the ethylene/air combustor.



Figure 4: All-quartz tubular reactor, shown with Inconel electrodes (scale in inches).



- |             |                   |                       |                       |
|-------------|-------------------|-----------------------|-----------------------|
| 1. cathode  | 2. cathode sleeve | 3. reactor outer wall | 4. anode              |
| 5. end plug | 6. gap holder     | 7. exit port          | 8. thermocouple port. |

Figure 5: Schematic of the all-quartz tubular reactor.



Figure 6: Fan-type plasma reactor (white box on right) shown with Japan-Inter uHV-10 AC power source and Yokogawa digital oscilloscope DL 1520, as used in experiments conducted at the University of Connecticut.

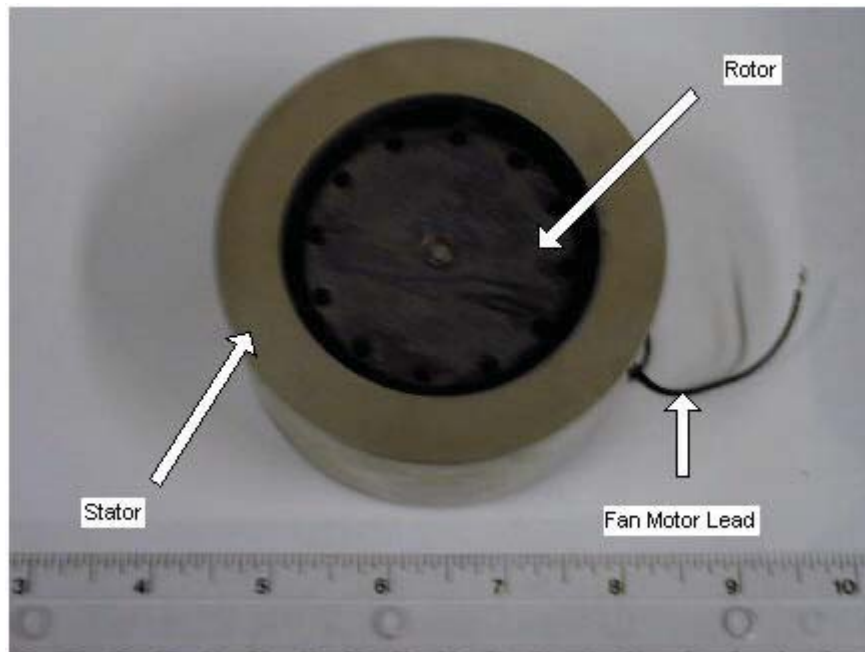


Figure 7: Fan-type plasma reactor removed from outer casing (scale in inches).

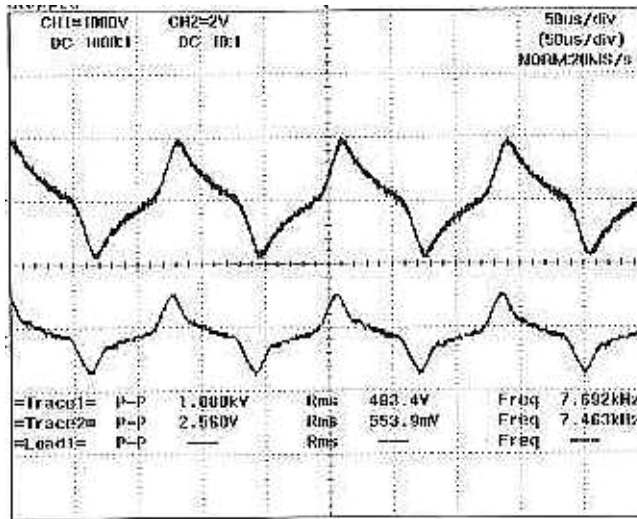


Figure 8: Waveform employed in fan-type plasma generator experiments. Waveform image was acquired from a Yokogawa digital oscilloscope DL 1520 used to monitor the setup.

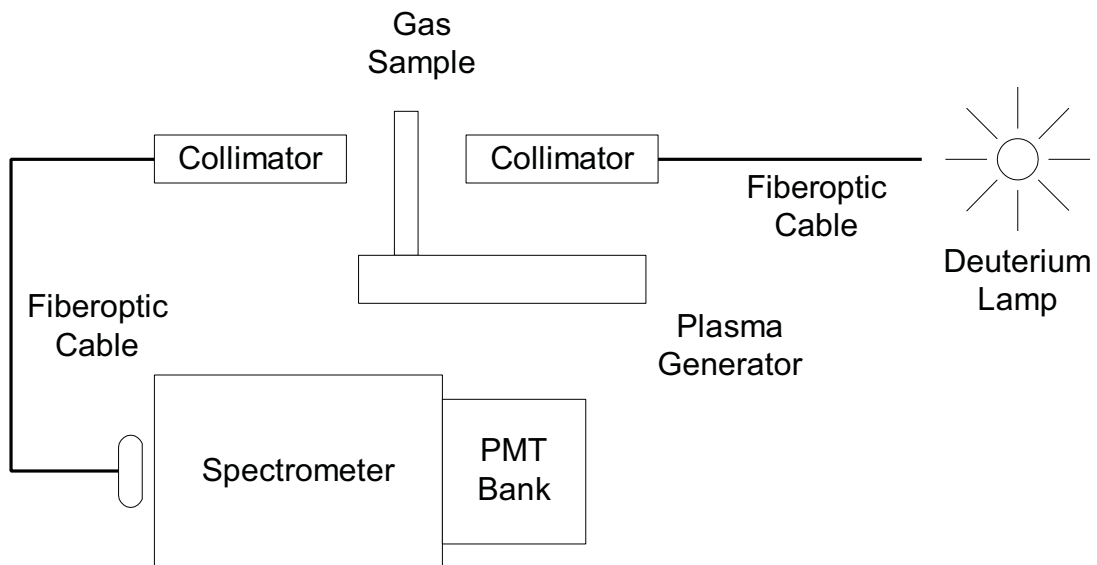


Figure 9: Configuration used for UV absorption measurement.

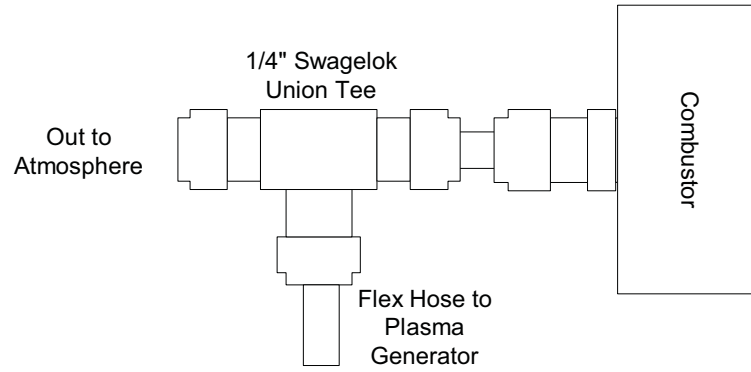


Figure 10: Schematic of modifications made to the combustor exit to avoid combustor instabilities during the experiments performed at the University of Connecticut.

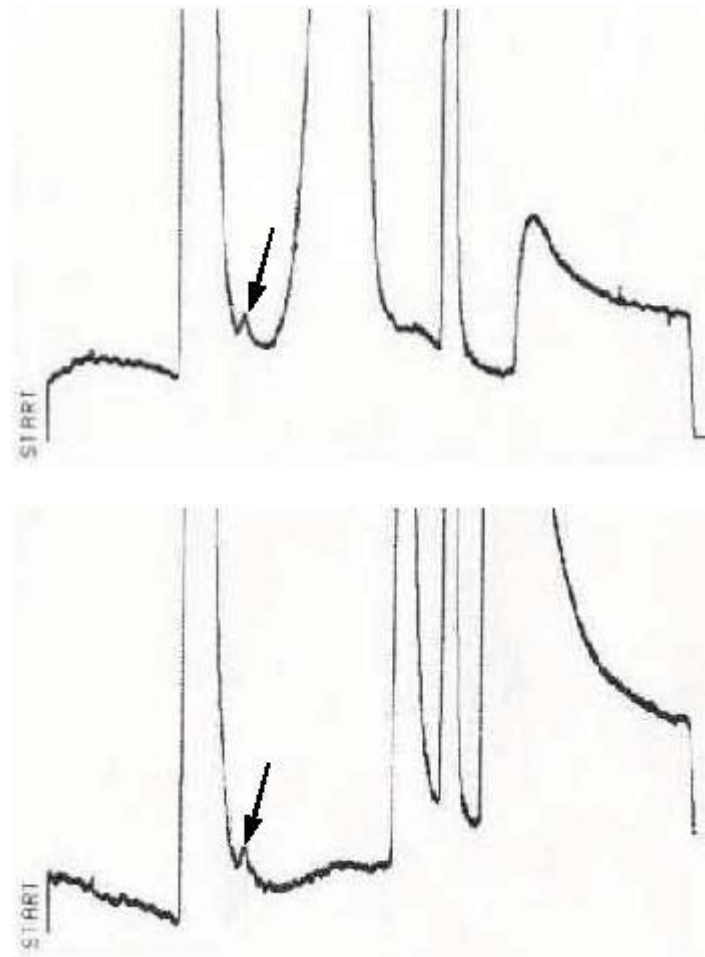


Figure 11: GC output data. Upper: data for plasma-off condition. Lower: data for plasma-on condition. Arrows are pointing to the peak corresponding to NO effusion from the GC column. Scales of the two plots are identical.

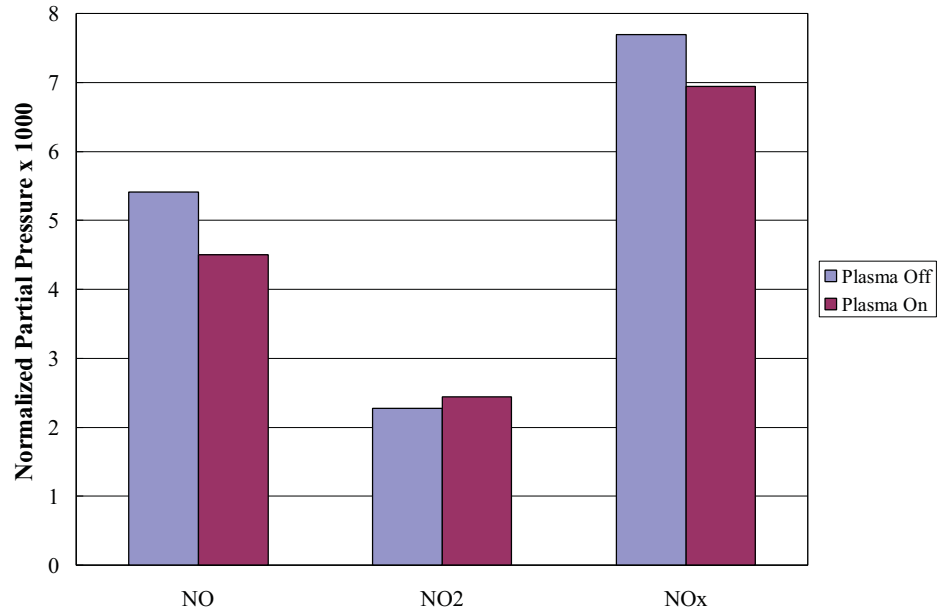


Figure 12: MS results for plasma-off and plasma-on conditions, including NO, NO<sub>2</sub> and NO<sub>x</sub> (NO + NO<sub>2</sub>).

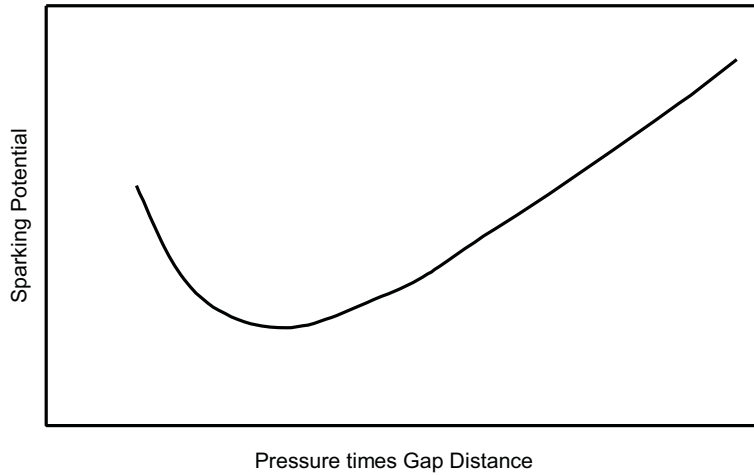


Figure 13: Paschen curve, relating required breakdown voltage to gas pressure times gap width for a typical gas. Both scales are logarithmic. Plot adapted from Ref. [19].

## References

1. Wark, K. and Warner, C. F., *Air Pollution: Its Origin and Control*, IEP, New York (1976).
2. Glassman, I., *Combustion*, 3 ed. Academic Press, New York (1996).
3. Shelef, M. and Graham, G. W., "Why Rhodium in Automotive Three-Way Catalysts," *Catal. Rev.-Sci. Eng.*, 38:433 (1994).
4. Marquez-Alvarez, C., Rodriguez-Ramos, I., Guerrero-Ruiz, A., Haller, G. L., and Fernandez-Garcia, M., "Selective Reduction of NO<sub>x</sub> With Propene Under Oxidative Conditions: Nature of the Active Sites on Copper-Based Catalysts," *J. Am. Chem. Soc.*, 119:2905 (1997).
5. Li, W., Sirilumpen, M., and Yang, R. T., "Selective Catalytic Reduction of Nitric Oxide by Ethylene in the Presence of Oxygen Over Cu<sup>2+</sup> Ion-Exchanged Pillared Clays," *Appl. Catalysis B: Environmental*, 11:347 (1997).
6. Feng, X. and Hall, W. K., "FeZSM-5: A Durable SCR Catalyst for NO<sub>x</sub> Removal from Combustion Systems," *J. Catalysis*, 166:368 (1997).
7. Armor, J. N., "Catalytic Removal of Nitrogen Oxides: Where Are the Opportunities?" *Catalysis Today*, 26:99 (1995).
8. Luo, J., Suib, S. L., Marquez, M., Hayashi, Y., and Matsumoto, H., "Decomposition of NO<sub>x</sub> with Low-Temperature Plasmas at Atmospheric Pressure: Neat and in the Presence of Oxidants, Reductants, Water, and Carbon Dioxide," *J. Phys. Chem. A*, 102:954 (1998).
9. Luo, J., Suib, S. L., Hayashi, Y., and Matsumoto, H., "Emission Spectroscopic Studies of Plasma-Induced NO Decomposition and Water Splitting," *J. Phys. Chem. A*, 103:6151 (1999).
10. Bathie, W. W., *Fundamentals of Gas Turbines*, 2 ed. Wiley, New York (1996).
11. Suib, S. L., Brock, S. L., Marquez, M., Luo, J., Matsumoto, H., and Hayashi, Y., "Efficient Catalytic Plasma Activation of CO<sub>2</sub>, NO, and H<sub>2</sub>O," *J. Phys. Chem. A*, 102:9661 (1998).
12. Brock, S. L., Marquez, M., Suib, S. L., Hayashi, Y., and Matsumoto, H., "Plasma Decomposition of CO<sub>2</sub> in the Presence of Metal Catalysts," *J. Catalysis*, 180:225 (1998).
13. Brock, S. L., Shimojo, T., Marquez, M., Marún, C., Suib, S. L., Matsumoto, H., and Hayashi, Y., "Factors Influencing the Decomposition of CO<sub>2</sub> in AC Fan-Type Plasma Reactors: Frequency, Waveform, and Concentration Effects," *J. Catalysis*, 184:123 (1999).
14. Huang, A., Xia, G., Wang, J., Suib, S. L., Hayashi, Y., and Matsumoto, H., "CO<sub>2</sub> Reforming of CH<sub>4</sub> by Atmospheric Pressure ac Discharge Plasmas," *J. Catalysis*, 189:349 (2000).
15. Wang, J., Xia, G., Huang, A., Suib, S. L., Hayashi, Y., and Matsumoto, H., "CO<sub>2</sub> Decomposition Using Glow Discharge Plasmas," *J. Catalysis*, 185:152 (1999).
16. Scire, J. J., Yetter, R. A., and Dryer, F. L., "Verification of Extractive NO Measurements by *in situ* UV Absorption Measurement," paper presented at the First Joint Meeting of the United State Sections of the Combustion Institute, Washington, DC, p. 188 (1999).

17. Lempert, W. R., "Microwave Resonance Lamp Absorption Technique for Measuring Temperature and OH Number Density in Combustion Environments," *Combust. Flame*, 73:89 (1988).
18. Alberty, R. A., *Physical Chemistry*, 7 ed., Wiley, New York (1987).
19. Jahn, R. G., *Physics of Electric Propulsion*, McGraw-Hill, New York (1968).